Journal of Power Sources 196 (2011) 1069–1077

Contents lists available at ScienceDirect

Journal of Power Sources

journal homepage: www.elsevier.com/locate/jpowsour

Alternative hybrid electrolytes based on a series of bis(trialkoxysilyl)alkanes and 3-(trihydroxysilyl)-1-propane sulfonic acid applied in gas diffusion electrodes of proton exchange membrane fuel cells

C.W. Lin*, L.C. Chung, R.S. Veerapur, F.C. Yang

Department of Chemical Engineering, National Yunlin University of Science and Technology, 123, Sec.3, University Road, Douliu, Yunlin 640, Taiwan

ARTICLE INFO

Article history:
Received 29 June 2010
Received in revised form 5 August 2010
Accepted 9 August 2010
Available online 17 August 2010

Keywords:
Fuel cell
Gas diffusion electrodes
Hybrid electrolytes
Catalyst layer
Microstructure

ABSTRACT

This study demonstrates a method for improving the electrolyte distribution in catalyst layers and enhancing the utilization of catalyst existing in primary pores. Bis(trialkoxysilyl)alkanes (BTAS-alkanes) and 3-(trihydroxysilyl)-1-propane sulfonic acid (THS)Pro-SO_3H) precursors have been used to prepare a series of hybrid electrolytes with various organic segment lengths of BTAS-alkanes and ratios of organic moiety and sulfonic acid groups. Investigations of BTAS-alkanes series includes bis(triethoxysilyl)octane (BTES-Oct), bis(trimethoxysilyl)hexane (BTMS-Hex), and bis(triethoxysilyl)ethane (BTES-Eth). Small angle X-ray spectroscopy (SAXS) identifies morphological phase separation in BTES-Oct and BTMS-Hex hybrid electrolytes. The results of mercury porosimetry and BET porosimetry show that the hybrid electrolytes have better capability than Nafion ionomer to penetrate into primary pores of the catalyst layers. Electrochemical measurements including electrode polarization, electrochemical active surface (EAS) and electrochemical impedance spectroscopy (EIS) are discussed. The BTES-Oct or BTMS-Hex hybrid electrolytes with higher ratio of organic moiety and sulfonic acid group have achieved better electrode performance. Oxygen benefit current (OBC) results indicate that higher ratios of BTES-Oct/(THS)Pro-SO_3H provides higher hydrophobicity with better gas transport properties. However, the hybrid electrodes exhibit lower cathode performance than Nafion®-based electrodes due to excessive electrolyte incorporated in the catalyst layer.

1. Introduction

Due to their higher power densities and environmental benefits, proton exchange membrane fuel cells (PEMFCs) have recently generated an enormous amount of research as alternative power sources for automotive, stationary, and portable applications. However, several issues must be addressed before PEMFC systems can be commercialized, including the use of expensive components with limited performance, and the poor durability of membrane electrode assemblies (MEAs). Ironically, low catalyst activity and mass transport limitations at the cathode leads to lower power density values. An optimized MEA configuration that includes a catalyst layer and gas diffusion layers (GDLs) could address these shortcomings [1–3]. MEA efficiency depends on three major factors: (i) amount of catalyst, (ii) type of proton exchange membrane (PEM), and (iii) gas diffusion layers (GDL) characteristics [4]. Among these factors, GDL characteristics play an important role in achieving high performance of PEMFC. The GDL acts as an effective path for the transport of gas reactants to the catalyst layer, exhibiting low electronic resistivity for the transmission of electrons. The GDL also act as a flexible surface with proper hydrophobicity preventing water flooding and providing better contact with neighboring components [5,6]. High PEMFC performance requires an optimal combination of electron transport, proton transport and mass transport [7]. The combination of these mechanisms forms a three-phase-boundary where electrochemical reactions occur [8,9].

One of the important goals in current PEMFC research is to address the basic understanding of both gas transport and ion transport. The transport of gas and ions occurs in different directions; gas diffuses perpendicularly to the ionomer thin film, while ions migrate parallel to it. Electrochemical reactions generally occur in the gas diffusion electrode (GDE). Because these reactions involve complicated factors, it is difficult to evaluate the influence of one parameter while keeping other properties constant. For example, a variation in the ionomer content simultaneously affects gas permeability, catalytic activity and ionic resistance [4–6]. Wilson et al. employed a thin-film method to improve the electrolyte distribution in catalyst layers. This approach enhances PEMFC performance

* Corresponding author. Tel.: +886 5 5342601 4613; fax: +886 5 5312071.
E-mail address: lincw@yuntech.edu.tw (C.W. Lin).

0378-7753/$ – see front matter © 2010 Elsevier B.V. All rights reserved.
doi:10.1016/j.jpowsour.2010.08.024

by increasing the number of Pt particles in contact with proton conducting networks, which in turn increases catalyst utilization [10–12]. The distribution of the three-phase-boundary is another critical phenomenon governed by the microstructures of catalyst layers. Recent study by Watanabe et al. shows that there are two types of pores in the catalyst layer: primary pores with a diameter of <0.1 μm and secondary pores with a diameter of >0.1 μm and more than 85% of Pt particles are located on the wall of primary pores [13,14]. Uchida et al., further analyzed pore structures in the PEMFC catalyst layer, showed that sulfonated polymer electrolytes could not penetrate into primary pores with small diameters [15,16]. This suggests that the catalyst utilization in primary pores is excluded from three-phase boundaries.

Recent research efforts have focused on the preparation of organic–inorganic hybrids through sol–gel processes [17–19]. These hybrids have the advantages of thermal stability provided by an inorganic backbone, while organic chains confer the required specific properties such as flexibility and processibility. These hybrid electrolytes become proton conducting when they are doped with acidic moieties such as monododecylphosphate (MDP) or 12-phosphotungstic acid (PWA) and a family of acid functionalized polysilsesquioxanes (Si_2O_3) [20,21]. Nishikawa et al. improved PEMFC performance by combining nano-hybrid electrolytes with platinum-loaded carbon blacks [22,23]. Our earlier reports investigate the feasibility of proton conducting hybrid membranes based on SiO_2/PEG (polyethylene glycol) doped with either 4-dodecylbenzene sulfonic acid (DBSA) or PWA as electrolytes in PEMFCs [24]. Continuing this line of research the present study demonstrates the preparation of various gas diffusion electrodes with a series of hybrid electrolytes through a sol–gel process involving BTAS-alkanes and (THS)Pro-SO_3H precursors. Mercury porosimetry and BET porosimetry measurements were performed to examine the variation of pore-size distribution before and after incorporating the hybrid electrolyte in catalyst layer as binder in advance to examine the possibility of utilization of catalysts located in the primary pores. The rational behavior between organic moieties and electrode performance were examined by varying the organic segment length of BTAS-alkane precursors. This study also compares the performance of the electrodes with the hybrid electrolytes and Nafion®. The outcome of these results indicates that the use of alternative organic–inorganic hybrid electrolyte may be advantageous in utilizing catalyst existing in primary pores of gas diffusion electrode.

2. Experimental

2.1. Preparation of electrodes

2.1.1. Hybrid electrolyte-based electrodes

Hybrid electrolytes were prepared via sol–gel process using BTAS-alkane (Gelest Co. Ltd., Japan) and (THS)Pro-SO_3H aqueous solution (Gelest Co. Ltd., Japan) precursors by varying the organic segment lengths of BTAS-alkanes viz., bis(triethoxysilyl)octane, bis(trimethoxysilyl)hexane and bis(triethoxysilyl)ethane with the number of carbon atoms in their organic moieties of 8, 6, and 2, respectively. Scheme 1 presents the structural formulas of precursors. This study adopts the hybrid electrolytes preparation procedure reported in the literature [22]. Pt-CB (Platinum nominally 50% on Carbon Black Alfa Aesar) and (THS)Pro-SO_3H were mixed with constant stirring for 2 h at room temperature. A BTAS-alkane and 2-propanol (>99.8%, Sigma–Aldrich, USA) mixture was added and once again stirred for 30 min. The mixing ratio of Pt:BTAS-alkane:(THS)Pro-SO_3H:water-IPA were 1:A:B:20 by weight. A uniform paste was spread onto commercial gas diffusion layers (Carbon cloth, 15 wt.% wet proofing, microporous layer on single side, type: CeW1S12, HEPHAS energy) with a circular area of 1 cm^2 and Pt loading of 0.5 mg cm^{-2}. The electrodes were dried under 60 °C and rinsed with deionized water before measurement.

2.1.2. Nafion®-based electrodes

Pt-CB and 2-propanol were mixed and until complete dispersion was achieved. Nafion® solution (5 wt.% Sigma–Aldrich, USA) was added this dispersion and again stirred to produce a uniform paste. The mixing ratio of Pt:IPA:Nafion® was 1:30:C [C representing Nafion® content (0.6, 1, 1.34, and 3)]. The paste was spread onto a commercial gas diffusion layer same as the one prepared in section 2.1.1 with a circular area of 1 cm^2 and Pt loading of 0.5 mg cm^{-2} then dried under 60 °C and rinsed with deionized water before measurements.

2.2. Small angle X-ray scattering measurements

A small angle X-ray scattering instrument (PSAXS-USH-WAXS-002, Osmic, USA) was used to determine the microstructures of the organic–inorganic hybrid electrolytes. BTAS-alkane, (THS)Pro-SO_3H and IPA (Sigma–Aldrich, USA) were mixed in equimolar amount at room temperature with constant stirring for 30 min. The aging process conducted at 60 °C and 95% R.H. for 12 h. After drying, the samples were ground into powder for SAXS measurement.

2.3. Porosimetry measurements

The pore-size distribution and the specific pore volume were calculated from an intrusion curve obtained by a mercury pore sizer (Autopore 9520, Micromeritics Corporate, USA). Mercury porosimetry technique could determine the distribution of pore diameter between 300 μm and 3 nm. The volume of mercury (V) penetrated into the pore is measured directly as a function of applied pressure. For mercury porosimetry, shredded hybrid electrolytes weighing 100–200 mg were subjected to an operating pressure of 0.10–60,000 psi. Intrusion of mercury began at a pressure of 0.44 psi.

The specific surface area and the pore volume distribution were also measured from BET porosimetry (Beckman Coulter SA3100, Taiwan). This type of pore sizer could determine the distribution of pore diameter in nanometer range. For BET porosimetry, hybrid electrolytes were crushed into powder weighed 100–200 mg for subsequent outgassing at approximately 150 °C for 2 h before measurement. Nitrogen adsorption/desorption was carried out at −196.15 °C.

2.4. Electrochemical measurements

Electrochemical measurements were conducted by a half-cell system based on a conventional three-electrode cell [25], and a potentiostat (Autolab, PGSTAT30, Eco Chemie, USA) was adopted to evaluate electrode performance. The prepared GDE was mounted on a PTFE holder to form a working electrode. The PTFE holder contained a Pt ring as current collector, and gases were fed from the back of the electrode. The reference electrode and counter electrode were Ag/AgCl and Pt wire, respectively. Scheme 2 shows the construction of the half-cell system. 0.5 M sulfuric acid was used as a liquid electrolyte for this system. When oxygen was fed into the working electrode, it reacted with the protons of sulfuric acid in an oxygen reduction reaction (ORR). Therefore, the proposed design simulated fuel cell cathode. This design can eliminate other variables while achieving the property of a freestanding GDE.

Three electrochemical measurements were used to evaluate the performances of various electrodes with the same catalyst but different electrolytic binder at room temperature. Galvanstatic

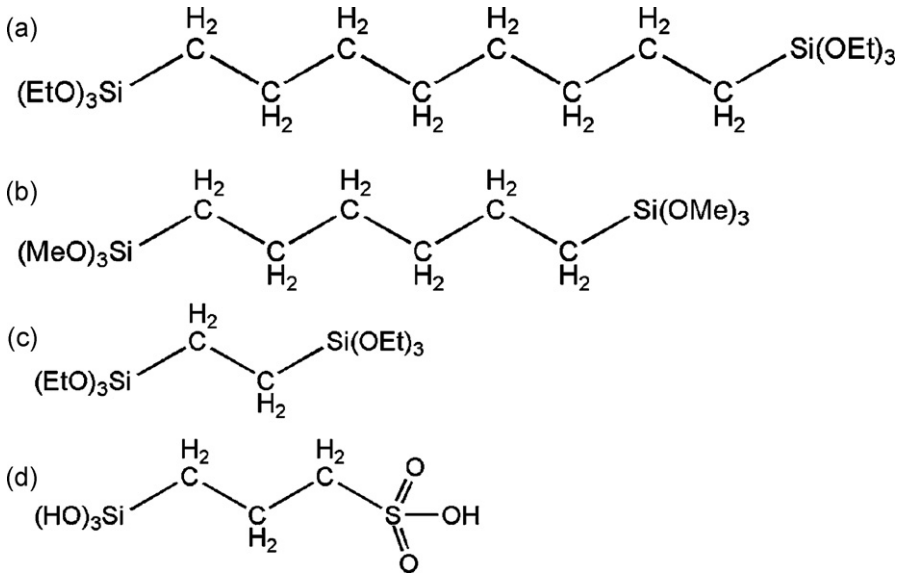

Scheme 1. Structural formulas of precursors. (a) BTES-Oct, (b) BTMS-Hex, (c) BTES-Eth and (d) (THS)Pro-SO_3H.

polarization (GP) was conducted in an oxygen and/or air atmosphere. Note that the potential values are referred to Ag/Agcl. Experimental conditions include a gas flow rate of 100 mL min^{-1}, a scan range of 1–0 V, and a scan rate of 40 mV s^{-1}. The polarization curve was obtained via GP analysis. Cyclic voltammetry (CV) was conducted in a nitrogen atmosphere. The gas flow rate was maintained at 100 mL min^{-1}, with a scan range of 0.2∼1 V and a scan rate of 40 mV s^{-1}. After recording 30 scans, the last cycle was considered as stable CV spectra. The peaks of hydrogen adsorption/desorption on Pt appeared at a range of 0.2–0.1 V. The total exchanged charges were calculated by evaluating the areas of hydrogen desorption peak and dividing it by the reference hydrogen adsorption charge (210 μC cm^{-2}) to determine the electrochemically active surface (EAS). The EAS represents the Pt area capable of hydrogen adsorption. Electrochemical impedance spectra (EIS) analysis was conducted in an oxygen or air atmosphere. The value of perturbation was 0.3 V. The gas flow rate was 100 mL min^{-1}, with an operating potential of 0.3 V and a frequency range of 10000–0.01 Hz.

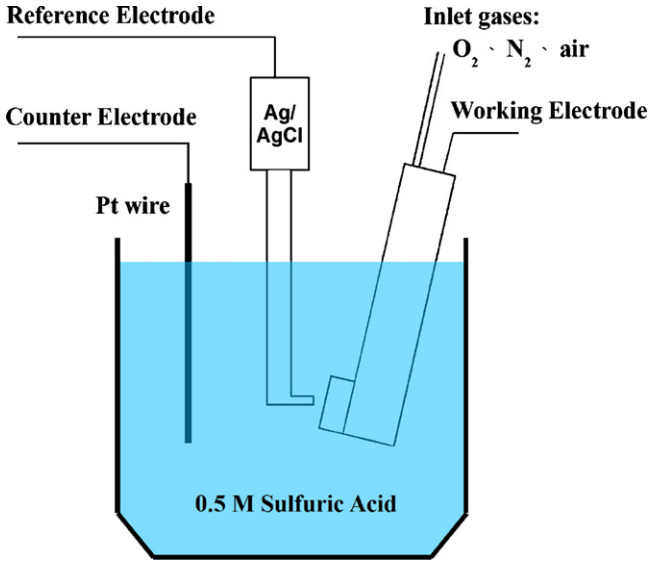

Scheme 2. Schematic representation of half-cell system.

3. Results and discussion

3.1. Small angle X-ray scattering measurements

Fig. 1 displays the SAXS spectra of hybrid electrolytes prepared with various BTAS-alkane precursors. In this study, the molar ratio of hybrid electrolytes was BTAS-alkane/(THS)Pro-SO_3H = 1. The BTMS-Hex and BTES-Oct-based hybrid electrolytes exhibited visible peaks, indicating phase separation in the microstructure of the hybrid electrolytes. The BTES-Eth-based hybrid electrolyte, did not exhibit a peak. This result clearly shows that precursors containing longer organic segment lengths, e.g. BTES-Oct and BTMS-Hex-based hybrid electrolytes, formed a microphase separation structure. However, due to their smaller organic segment lengths, BTES-Eth-based hybrid electrolytes could not form a microphase separation structure. The d-spacing of hybrid electrolytes, i.e., the distance between inorganic-rich phases, were 36.4 nm and 28.3 nm for the BTES-Oct and BTMS-Hex- based hybrid electrolytes, respectively. In other words, the distance between inorganic-rich phases was the size of the organic-rich phase.

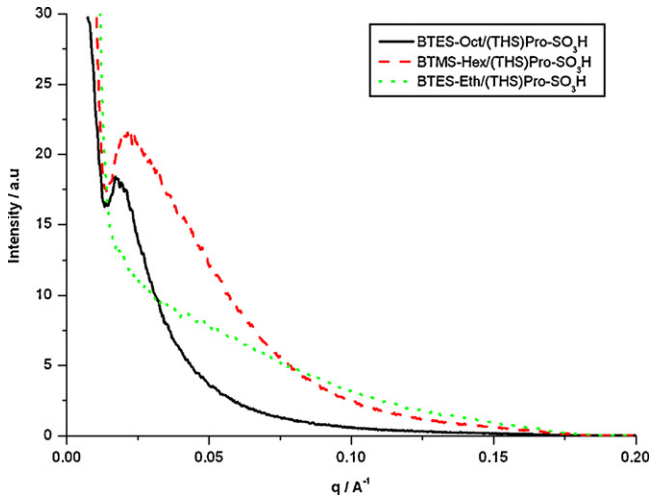

Fig. 1. SAXS spectra of BTES-Eth, BTMS-Hex and BTES-Oct-based hybrid electrolytes.

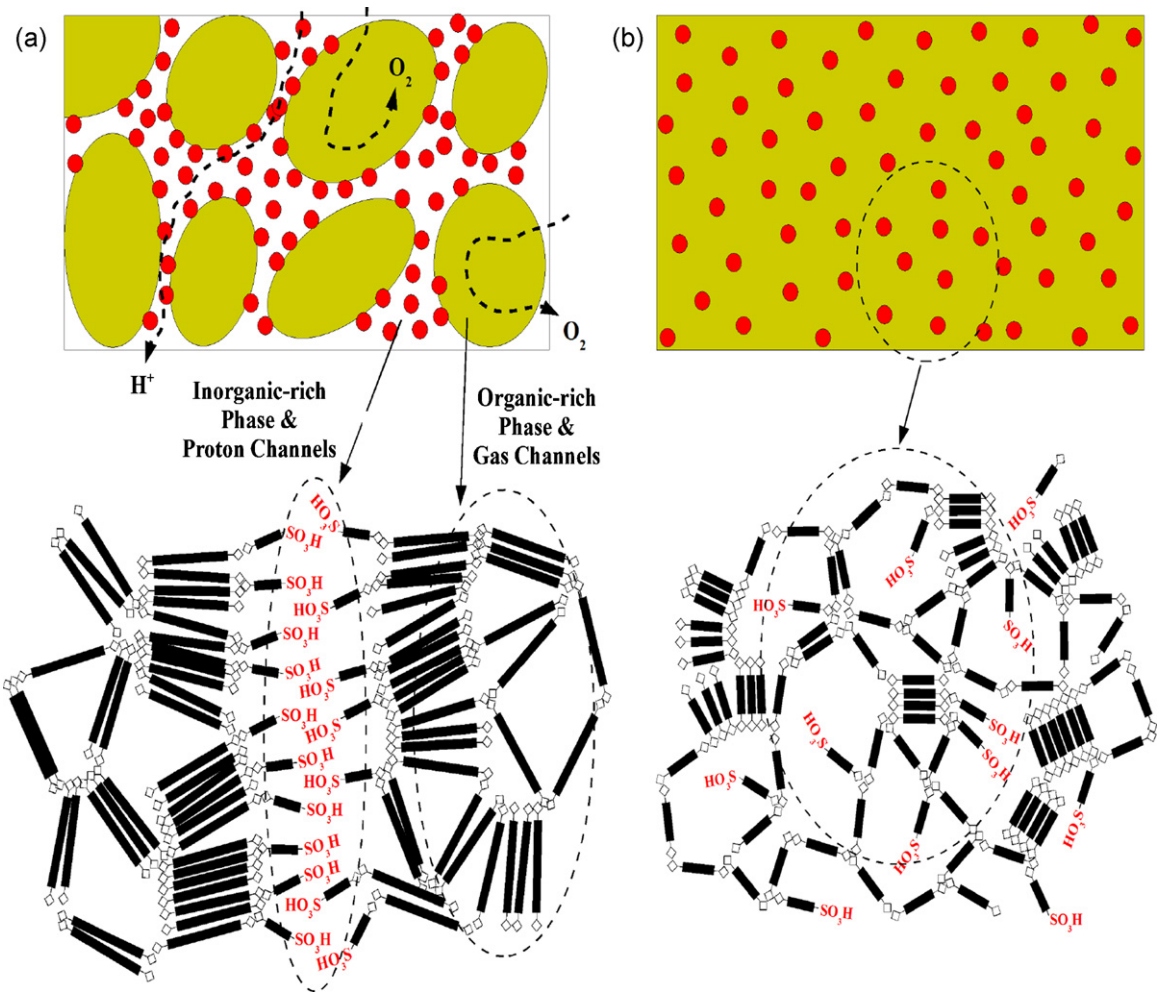

Fig. 2. Phase separation morphology of (a) BTES-Oct and BTMS-Hex (b) BTES-Eth-based hybrid electrolytes.

Fig. 2 shows the SAXS measurements of the model phase separation structure. This figures show that hybrid electrolytes based on BTES-Oct and BTMS-Hex formed a microphase separation structure consisting of organic-rich phases and inorganic-rich phases. Fig. 2(a) suggests that the hydrophobic organic-rich phases provided transport channels for reactant gases, and that hydrophilic sulfonic groups were located in inorganic-rich phases. This kind of phase separation structure promotes transport properties in the catalyst layer because it provides independent transport channels for both gases and protons. Varying the organic segment length of the hybrid electrolytes changed the number of microphase. Because BTES-Eth-based hybrid electrolytes exhibit no phase separation structure, their protons, and gases show poor transportation [Fig. 2(b)].

3.2. Porosimetry measurements

Gas sorption (e.g. BET) and mercury porosimetry can be complementary techniques used in this study. Physical adsorption techniques can extend the lower size measurement down to about 0.35 μm diameter, thus probing well the variation of intra-particle microstructure due to penetration of organic–inorganic hybrid electrolytes. Mercury porosimetry was paired with the gas sorption technique in this study to obtain porosity information in the large size range (typically greater than about 0.3 μm diameter), which is not attainable by gas sorption.

3.2.1. BET porosimetry

Fig. 3 depicts the BET porosimetry measurements. These measurements revealed that the pore diameter of the catalyst layer in the hybrid electrolytes ranged from <100 nm. These results suggest that BTES-Eth-based hybrid electrolytes with smaller organic segment length produce no benefit in occupying primary pores.

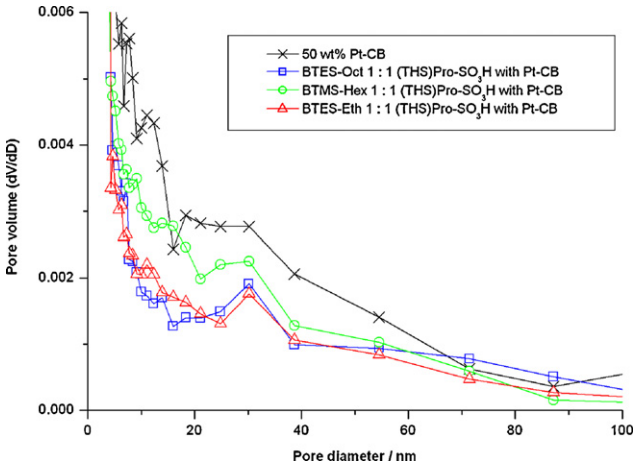

Fig. 3. BET porosimetry of hybrid electrolytes prepared using precursors with varying organic segment lengths.

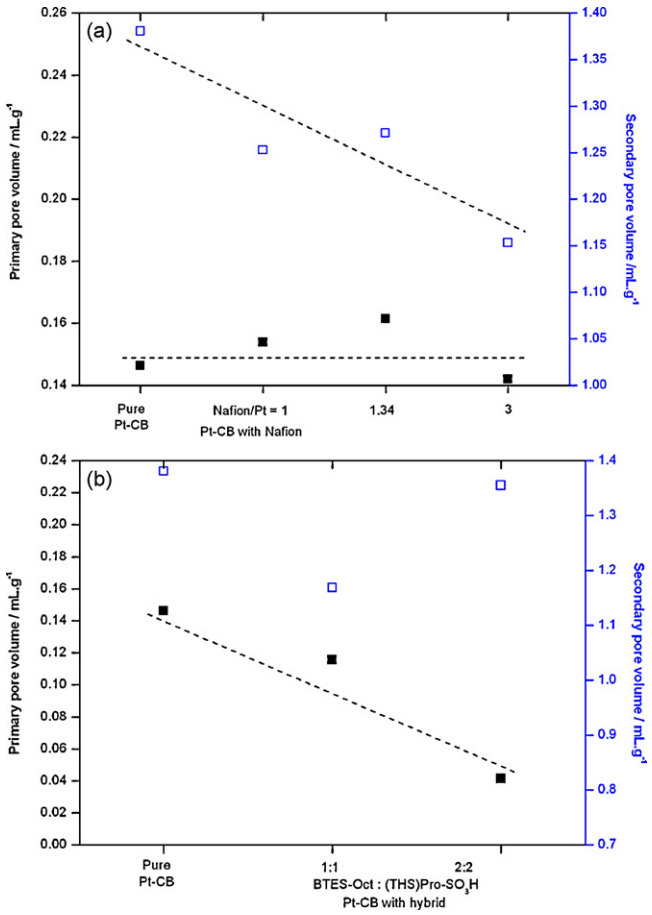

Fig. 4. Pore distributions with varying hybrid electrolyte contents by mercury porosimetry. (■) Primary pore and (□) secondary pore, (a) Nafion® and (b) TES-Oct/(THS)Pro-SO_3H.

3.2.2. Mercury porosimetry

The distribution of hybrid electrolytes in primary or secondary pores was determined specifically by mercury porosimetry. The Pt-CB (50 wt. %) has a pore boundary of 62.5 nm between primary and secondary pores. Fig. 4(a) and (b) shows the distribution of primary and secondary pores with varying contents of Nafion® and BTES-Oct-based hybrid electrolyte, respectively. An increase

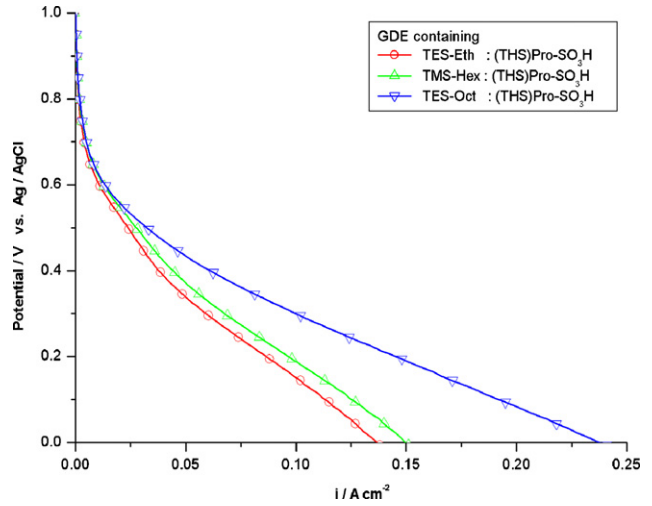

Fig. 5. Polarization curves of the GDEs containing various BTAS-alkanes with different organic segment lengths (C = 8, 6, and 2).

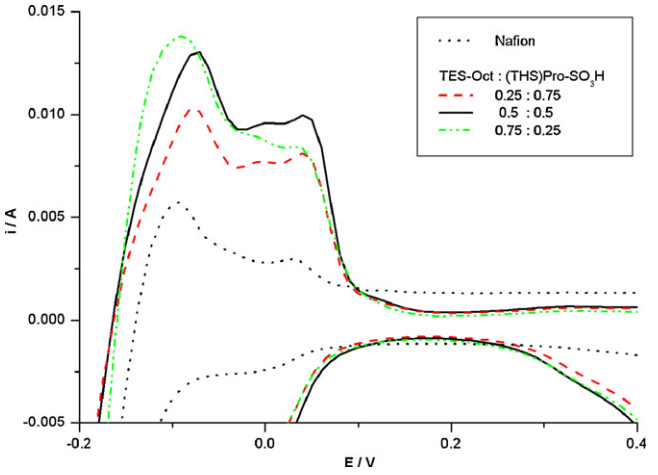

Fig. 6. Comparison of EAS of the electrodes based on the hybrid electrolyte BTES-Oct and Nafion, respectively.

in Nafion® content merely decreased the distribution of secondary pores. Increasing the content of BTES-Oct-based hybrid electrolyte affected the penetration of primary and secondary pores in the microstructure distribution. However, the primary pore population decreased substantially. These observations suggest that the BTES-Oct based hybrid electrolyte successfully occupied primary pores. Nafion® occupied only secondary pores, and failed to utilize the Pt catalyst existing in the primary pores. Fig. 4(b) shows that the secondary pore volume decreases after incorporating BTES-Oct-based hybrid electrolyte at BTES-Oct:(THS)Pro-SO_3H = 1:1. However, it rises again after changing content of the BTES-Oct-based electrolyte at BTES-Oct:(THS)Pro-SO_3H = 2:2. As the organic–inorganic hybrid has a highly porous nature, we presume the increase of secondary pore volume might be attributed to the porosity created by the hybrid electrolyte itself.

3.3. Influence of organic segment lengths of precursors on electrode performance

3.3.1. Polarization curves

Polarization curves, electrochemical active surface (EAS) values, and electrochemical impedance spectroscopy (EIS) values are the key factors in evaluating GDE performance. The total weight of hybrid electrolytes in the electrodes remained constant, while the lengths of organic segments based on BTAS-alkanes were varied. The amount of (THS)Pro-SO_3H was a variable. Fig. 5 shows the polarization curves of the GDEs containing various BTAS-alkanes with different organic segment lengths (C = 8, 6, and 2) at a ratio of BTAS-alkane:(THS)Pro-SO_3H equal to 0.5:0.5. The BTAS-alkanes-based hybrid electrolytes with longer organic segment lengths, i.e., BTES-Oct or BTMS-Hex, exhibited better polarization characteristics. The electrodes consisting of BTES-Oct-based hybrid electrolytes exhibited better performance with increasing BTES-Oct/(THS)Pro-SO_3H ratio. Increasing the organic moiety content produced similar trends, enhancing electrode performance.

3.3.2. Electrochemical active surface (EAS)

Fig. 6 shows a comparison of EAS of the electrodes with identical catalyst but based on the hybrid electrolyte BTES-Oct and Nafion, respectively. These results confirm our speculation that the BTES-Oct-based electrolyte can efficiently increase the catalyst utilization compared to Nafion-based electrode. Fig. 7 shows the influence of organic segment lengths on EAS of the electrodes with identical catalyst. EAS values describe the size of the interface between catalyst surfaces and the proton conducting network.

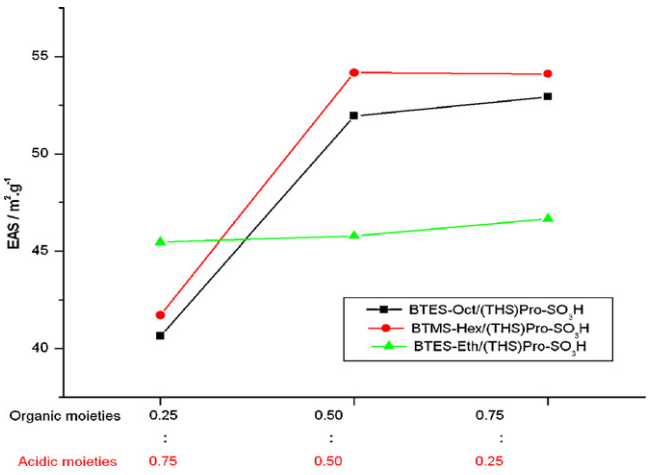

Fig. 7. Effect on EAS with varying precursors and its compositions.

The EAS values of BTES-Eth-based hybrid electrolytes suggest that with smaller organic segment lengths were ineffective in improving electrode performance. As the organic segment lengths increased, the EAS values of hybrid electrolytes based on BTES-Oct and BTMS-Hex increased substantially, along with the organic moiety content. Hybrid electrolytes containing rich sulfonic groups showed lower EAS. The effect of a higher hydrogen concentration was limited, suggesting that relatively few sulfonic groups were located at catalyst sites. This is due to BTAS-alkanes hybrid electrolytes, which act as the building blocks of macromolecules. The hybrid electrolytes in this study formed large macromolecular structures in the presence of abundant BTAS-alkanes. The organic moieties in precursors served as pillars to support macromolecular structures, and the functionality of two alkoxysilyl groups on BTAS-alkanes promoted the growth of macromolecular structures. The resulting hybrid electrolytes exhibited a widely expanded structure, with sulfonic groups covalently bonded on the macromolecules to attain good distribution in the catalyst layer. The distribution of sulfonic groups produced a larger proton conducting network, generating more EAS with Pt particles. For instance, BTAS-alkanes containing smaller organic segment lengths, i.e., hybrid electrolytes based on BTES-Eth, were poor building blocks for macromolecules, and produced oligomers instead. Poor distribution of sulfonic groups may result in decreased EAS values. In addition, the organic segments in BTES-Eth-based hybrid electrolytes were too short to serve as building blocks.

3.3.3. *Electrochemical impedance spectroscopy (EIS)*

Fig. 8 shows the EIS values of BTAS-alkane hybrid electrolytes. The frequency distributions of the impedances exhibited a semi-circular pattern. Lower impedances appeared in hybrid electrolytes based on BTES-Oct and BTMS-Hex, which had increased organic moieties in their networks. The hybrid electrolytes based on BTES-Oct and BTMS-Hex, exhibited larger impedances in the lower frequency region. However, the frequency distribution changed to a semi-circular pattern as the sulfonic acid group content increased. The increase in impedances in the lower frequency region represents limited oxygen transport. This retardation of oxygen transport in the catalyst layer caused a new arc in the lower frequency region, increasing impendence. When the two arcs were too close, they seemed to merge into once arc [26,27].

To demonstrate the relationship between oxygen transport and low-frequency impedance, this study presents EIS measurements with gas feeding of oxygen and air for the same electrode. Fig. 9 presents the resulting data which shows that a decrease in oxygen concentration enhanced low-frequency impedance, especially

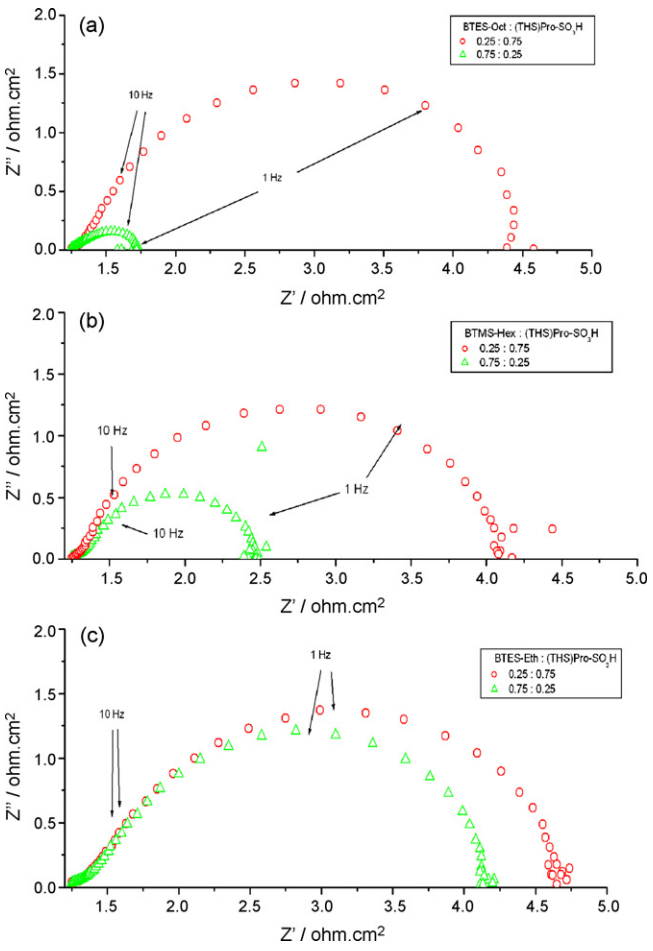

Fig. 8. EIS of hybrid electrolyte-based electrodes (a) BTES-Oct, (b) BTMS-Hex, and (c) BTES-Eth. Gas flow rate O_2 100 mL min^{-1}.

for electrode with high sulfonic acid group content. For an electrode sample of 0.25:0.75, impedance of 1 Hz was located at left side of this arc. This convinces that low-frequency impedances induce a considerable contribution to the whole impedance semi-circle. For electrodes based on hybrid electrolytes with higher sulfonic acid content, oxygen transport was responsible for the control of reaction kinetics.

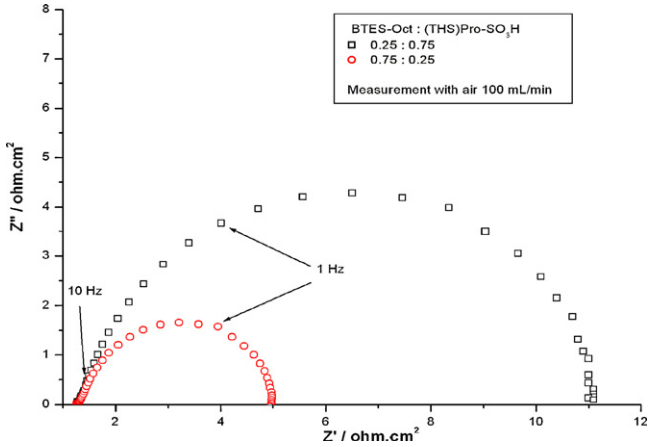

Fig. 9. EIS of BTES-Oct with different compositions under air. Gas flow rate 100 mL min^{-1}.

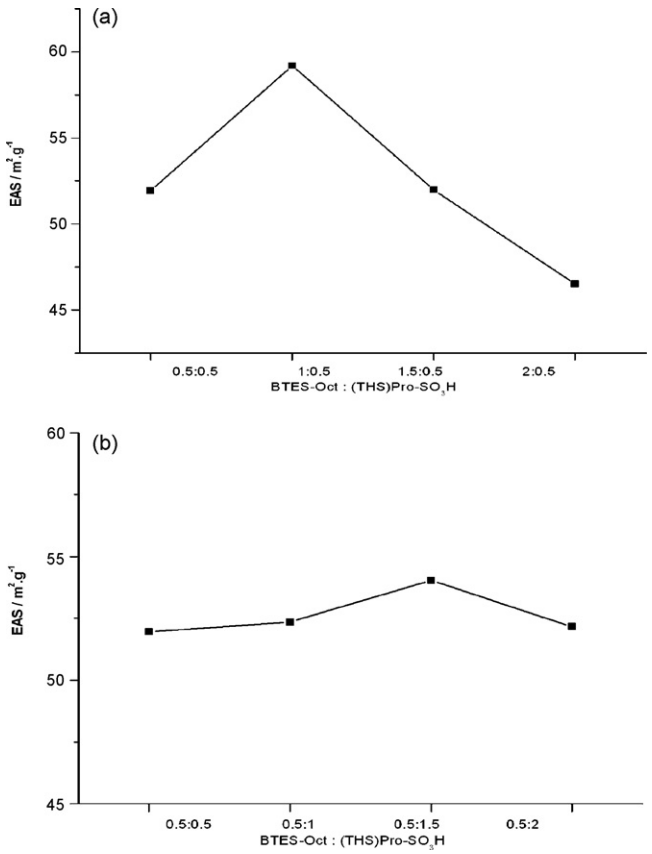

Fig. 10. EAS of BTES-Oct/(THS)Pro-SO_3H. (a) Increase of BTES-Oct and (b) increase of (THS)Pro-SO_3H.

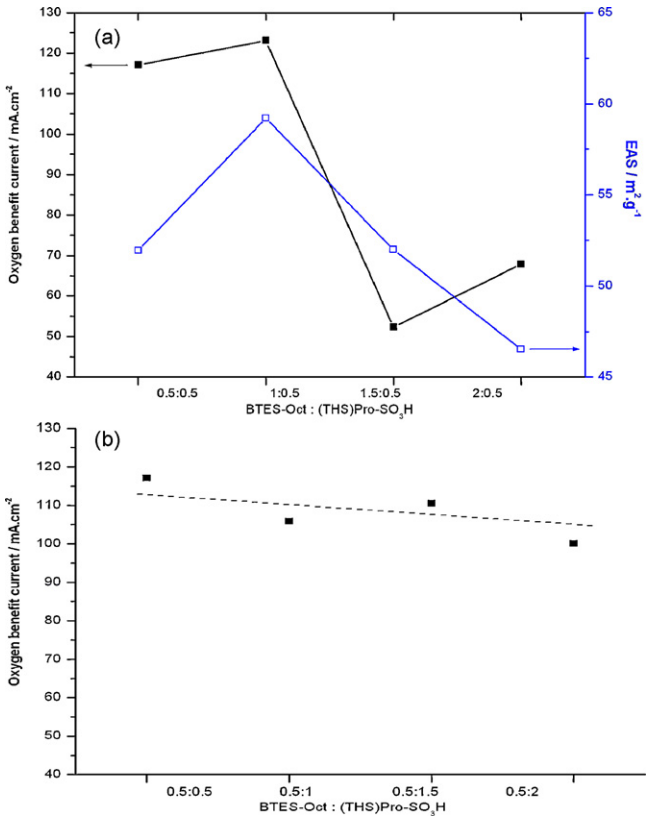

Fig. 11. Oxygen benefit current of BTES-Oct/(THS)Pro-SO_3H. (a) Increase of BTES-Oct and (b) increase of (THS)Pro-SO_3H.

3.4. Influence of organic moieties and sulfonic groups on performance of electrodes

In Section 3.3.1, the electrode with BTES-Oct based electrolyte exhibited a greater performance than other electrodes. When the contents of BTES-Oct and (THS)Pro-SO_3H precursors were increased, the electrode was improved in its performance. These results agree with data obtained by single cell test [22,23]. The most favorable ratio of BTES-Oct to (THS)Pro-SO_3H was 0.5:1, when hybrid electrolytes contained a higher amount of (THS)Pro-SO_3H.

The observations in Fig. 10(a) and (b) clearly show that the BTES-Oct content had remarkable influence on EAS. The BTES-Oct electrolyte as molecular frame promoted the distribution of sulfonic acid groups to effect in highest EAS values for BTES-Oct:(THS)Pro-SO_3H = 1:0.5 compositions. The excess amount of BTES-Oct electrolyte decreased the EAS because the concentrations of sulfonic acid groups decreased. Hence, with the increase of (THS)Pro-SO_3H content, EAS values raised slightly.

Introducing an oxygen benefit current (OBC) demonstrated the hydrophobic channels formed by organic moieties promoting gas transport in catalyst layers. Lower OBC values led to good gas diffusion in the catalyst layer. In other words, the performance of electrode does not rely on oxygen concentration heavily [10,27]. Fig. 11(a) and (b) shows that an increase of BTES-Oct electrolyte content decreased OBC values. However, OBC remained at about 100 mA cm^{-2} when the (THS)Pro-SO_3H electrolyte content increased. The OBC values exhibited by electrodes of composition BTES-Oct:(THS)Pro-SO_3H = 1:0.5 yields highest EAS that suggests more reaction sites needing oxygen. The higher BTES-Oct electrolyte content promotes transport of reactant gases, wherein OBC value was restrained at the same level. The electrodes of BTES-Oct:(THS)Pro-SO_3H = 0.5:0.5 and 1.5:0.5 have similar EAS, but with excess BTES-Oct electrolyte content, half of OBC is reduced. Fig. 12 compares the impedances of electrodes of compositions BTES-Oct:(THS)Pro-SO_3H = 1:0.5 and 0.5:1. Lower impedances in the low-frequency region appeared for electrode of BTES-Oct:(THS)Pro-SO_3H = 1:0.5. Both EIS analysis and information of OBC indicate that increase of organic moiety content promoting gas transport inside the catalyst layer.

With reference to results above, two competing mechanisms can be observed inside the electrodes, i.e., gas transport and proton transport. The excess BTES-Oct electrolyte content promoted reactant gas transport but caused lesser sulfonic group concentration inside the electrolyte. However, the excess (THS)Pro-SO_3H elec-

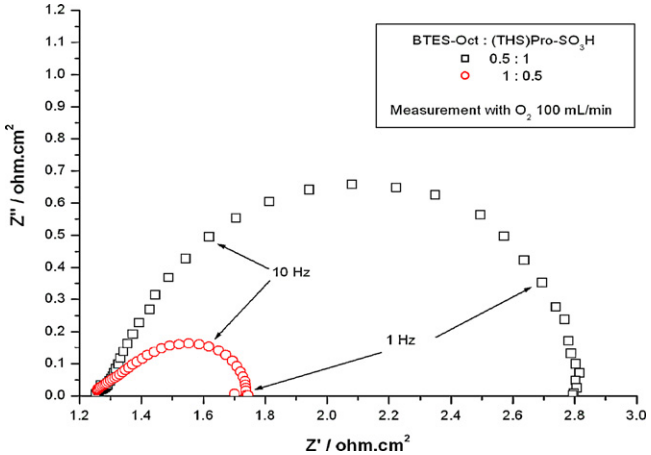

Fig. 12. EIS of BTES-Oct-based electrode of composition (0.5:1 and 1:0.5) at the gas flow rate O_2 100 mL min^{-1}.

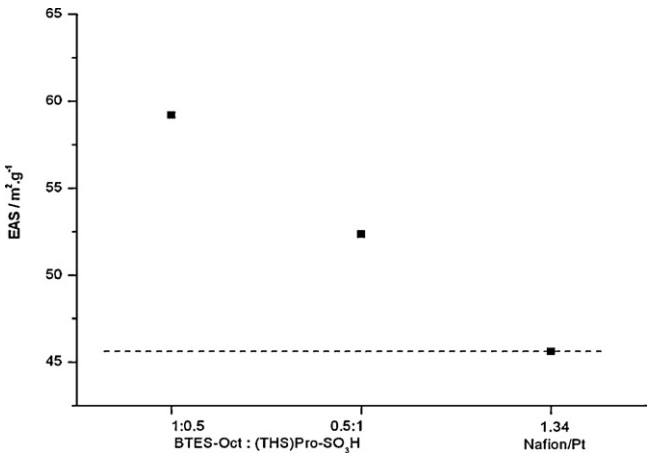

Fig. 13. EAS comparison of hybrid electrolytes-based electrodes and Nafion®-based electrodes.

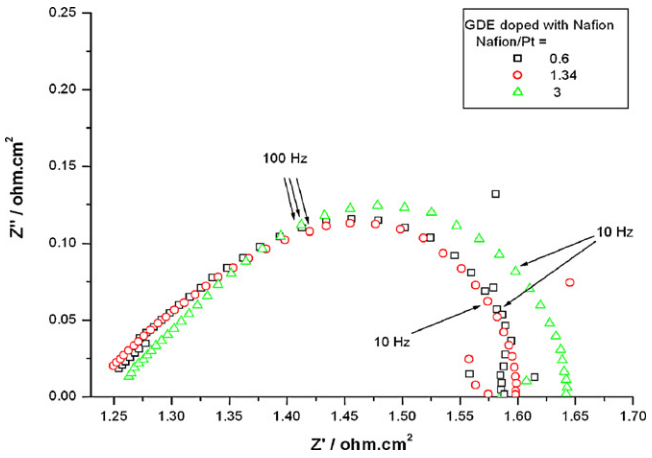

Fig. 15. Effect of Nafion® content on EIS.

trolyte content magnified proton conducting network but caused pore flooding and hindered gas transport. Hence, the gas transport in electrodes containing hybrid electrolytes is a more efficient mechanism to enhance electrode performance.

3.5. Comparison of electrodes based on hybrid electrolytes and Nafion®-based electrodes

This study systematically compares the performance of the electrodes based on hybrid electrolytes and Nafion®-based electrode. Fig. 13 demonstrates the EAS values of electrodes based on the hybrid electrolytes (BTES-Oct: (THS)Pro-SO_3H = 1:0.5 and 0.5:1) and the Nafion® ionomer. The electrodes based on BTES-Oct hybrid electrolytes exhibited higher EAS than Nafion®-based electrode, with a maximum increase of 29.7%. However, the catalyst utilization increased due to penetration of hybrid electrolytes into primary pores. However, high catalyst utilization was not accompanied with high electrode performance. Fig. 14 shows that the Nafion®-based electrode exhibits better performance than the electrodes based on the organic–inorganic hybrid electrolytes.

Fig. 15 shows that the Nafion® content greatly influences the impedance of electrodes. Increasing the Nafion® content in electrodes increased the diameter of impedance semi-circle. However, low-frequency impedances showed no significant differences. The Nafion®-based electrodes reserved plenty of primary pores as the main channels of reactant gases. Electrodes based on hybrid electrolytes exhibited much smaller pores. As a result, the performance of electrodes based on hybrid electrolytes was found to be sensitive to gas transport. Even though electrodes based on hybrid electrolytes exhibited increased catalyst utilization, their lack of gas transport channels decreased their three-phase-boundaries. Therefore, the performance of electrodes achieved lower performance than Nafion®-based electrode.

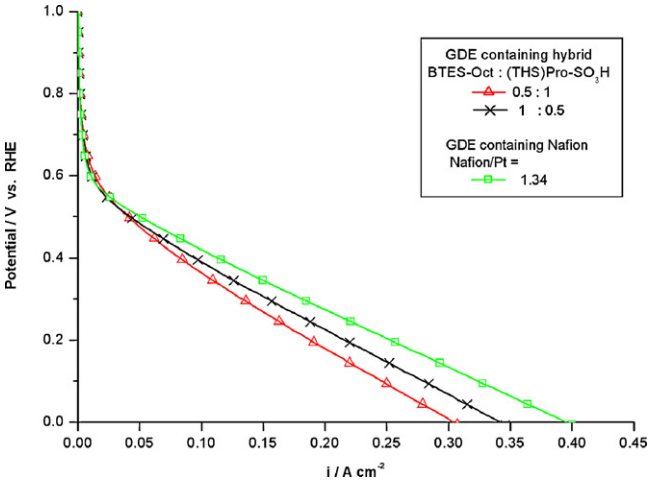

Fig. 14. Comparison of polarization curves of hybrid electrolytes-based electrodes and Nafion®-based electrodes.

4. Conclusion

This study reports a new approach to prepare gas diffusion electrode for PEMFC applications by using organic–inorganic hybrid electrolytes. Results showed that the electrodes based on BTAS-alkane/(THS)Pro-SO_3H hybrid electrolytes achieved greater extent of penetration into primary pores than Nafion®-based electrodes. The electrodes based on BTES-Oct hybrid electrolytes exhibited higher EAS than Nafion®-based electrode, with a maximum increase of 29.7%. The precursors containing longer organic segment lengths formed phase separation during the formation of nanostructure. The electrodes based on BTES-Oct hybrid electrolytes exhibited better polarization characteristics than BTMS-Hex and BTES-Eth hybrid electrolytes. Although the current approach efficiently enhanced catalyst utilization, a comparison of the electrode performances showed that the hybrid electrolyte were still inferior to the Nafion® ionomer in polarization characteristics. EIS measurements showed that the electrodes based on hybrid electrolytes lacked gas transport channels because the hybrid electrolytes penetrated the pores of the catalyst layer to an excessive extent. This implied novel technique in preparing electrodes with the alternative electrolytes needs to be further studied to achieve optimization.

Acknowledgement

This work is financially supported by the National Science Council of Taiwan, ROC (Grant No. NSC-98-2221-E-224-038).

References

[1] J. Larminie, A. Dicks, Fuel Cell Systems Explained, Wiley, UK, 2000.
[2] C. Yang, P. Costamagna, S. Srinivasan, J. Benziger, A.B. Bocarsly, J. Power Sources 103 (2001) 1–9.
[3] P. Costamagna, C. Yang, A.B. Bocarsly, S. Srinivasan, Electrochim. Acta 47 (2002) 1023–1033.
[4] H.Y. Chang, C.W. Lin, J. Membr. Sci. 218 (2003) 295–306.
[5] W. Mérida, D.A. Harrington, J.M. Le Canut, G. McLean, J. Power Sources 161 (2006) 264–274.
[6] E. Antolini, R.R. Passos, E.A. Ticianelli, J. Power Sources 109 (2002) 477–482.

[7] R. Thangamuthu, C.W. Lin, J. Power Sources 161 (2006) 160–167.
[8] A.M. Kannan, D. Parker, S. Sadananda, L. Munukutla, J. Wertz, J. Power Sources 178 (2008) 231–237.
[9] T.F. Hung, J. Huang, H.J. Chuang, S.H. Bai, Y.J. Lai, Y.W. Chen-Yang, J. Power Sources 184 (2008) 165–171.
[10] M.S. Wilson, S. Gottesfeld, J. Electrochem. Soc. 139 (1992) 28–30.
[11] M.S. Wilson, S. Gottesfeld, J. Appl. Electrochem. 22 (1992) 1–7.
[12] M.S. Wilson, US Patent No. 5234777, 1993.
[13] M. Watanabe, M. Tomikawa, S. Motoo, J. Electroanal. Chem. 182 (1985) 193–196.
[14] M. Uchida, Y. Aoyama, N. Eda, A. Ohta, J. Electrochem. Soc. 142 (1995) 4143–4149.
[15] M. Uchida, Y. Fukuoka, Y. Sugawara, N. Eda, A. Ohta, J. Electrochem. Soc. 143 (1996) 2245–2252.
[16] M. Uchida, Y. Aoyama, N. Eda, A. Ohta, J. Electrochem. Soc. 142 (1995) 463–468.
[17] J.E. Mark, C.Y.C. Lee, P.A. Bianconi (Eds.), Hybrid Organic–Inorganic Composites, ACS, Washington, DC, 1995.
[18] J.E. Mark, Heterogen. Chem. Rev. 3 (1996) 307–326.
[19] M. Popall, M. Andrei, J. Kappel, J. Kron, K. Olma, B. Olsowski, Electrochim. Acta 43 (1998) 1155–1161.
[20] I. Honma, H. Nakajima, O. Nishikawa, T. Sugimoto, S. Nomura, Solid State Ionics 162 (2003) 237–245.
[21] I. Honma, S. Nomura, H. Nakajima, J. Membr. Sci. 185 (2001) 83–94.
[22] O. Nishikawa, T. Sugimoto, S. Nomura, K. Doyama, K. Miyatake, H. Uchida, M. Watanabe, Electrochim. Acta 50 (2004) 667–672.
[23] O. Nishikawa, K. Doyama, K. Miyatake, H. Uchida, M. Watanabe, Electrochim. Acta 50 (2005) 2719–2723.
[24] R. Thangamuthu, C.W. Lin, Solid State Ionics 176 (2005) 531–538.
[25] Y.F. Huang, L.C. Chuang, A.M. Kannan, C.W. Lin, J. Power Sources 186 (2009) 22–28.
[26] J.M. Song, S. Suzuki, H. Uchida, M. Watanabe, Langmuir 22 (2006) 6422–6428.
[27] V.A. Paganin, C.L.F. Oliveira, E.A. Ticianelli, T.E. Springer, E.R. Gonzalez, Electrochim. Acta 43 (1998) 3761–3766.